J|A|C|S
ARTICLES

Published on Web 06/24/2010

Bimodal Polarons and Hole Transport in Poly(3-hexylthiophene):Fullerene Blend Films

Jiamo Guo,[†] Hideo Ohkita,*[,†,‡] Seiichirou Yokoya,[†] Hiroaki Benten,[†] and Shinzaburo Ito[†]

Department of Polymer Chemistry, Graduate School of Engineering, Kyoto University, Katsura, Nishikyo, Kyoto 615-8510, Japan and PRESTO, Japan Science and Technology Agency (JST), 4-1-8 Honcho Kawaguchi, Saitama 332-0012, Japan

Received December 25, 2009; E-mail: ohkita@photo.polym.kyoto-u.ac.jp

Abstract: The bimolecular recombination dynamics in blend films of poly(3-hexylthiophene) (P3HT) and [6,6]-phenyl-C_{61}-butyric acid methyl ester (PCBM) has been studied by transient absorption spectroscopy. On a microsecond time scale, two polaron bands were observed at 700 and 1000 nm and exhibited different bimolecular recombination dynamics. The 700-nm band decayed with a time-independent bimolecular recombination rate of 10^{-12} cm^3 s^{-1}. The activation energy was as small as ~0.078 eV independently of the carrier density. On the other hand, the 1000-nm band decayed with a time-dependent bimolecular recombination rate, which varied from 10^{-12} to 10^{-13} cm^3 s^{-1}, depending on time or carrier density. The activation energy decreased exponentially from 0.178 to 0.097 eV with the increase in the carrier density. Therefore, we assigned the 700-nm band to freely mobile delocalized polarons in crystalline P3HT domains and the 1000-nm band to localized polarons trapped in relatively disordered P3HT domains. At a charge density of 10^{17} cm^{-3}, which corresponds to 1 sun open-circuit condition, some localized polarons exhibited trap-free bimolecular recombination due to trap-filling. These findings suggest that not only delocalized polarons but also some localized polarons play a crucial role in the efficient hole transport in P3HT:PCBM solar cells.

1. Introduction

Blend films of a conjugated polymer and [6,6]-phenyl-C_{61}-butyric acid methyl ester (PCBM) have received extensive attention in recent years for the potential applications in plastic solar cells.[1−3] Among them, polymer solar cells employing a blend film of poly(3-hexylthiophene) (P3HT) and PCBM as an active layer have been intensively studied and have exhibited power conversion efficiencies of 4−5% with relatively high fill factors close to 0.7 and external quantum efficiencies (EQEs) exceeding 80%. These device parameters are still among the highest in organic solar cells.[4−7] In such solar cells, the short-circuit current density (J_{SC}) increases linearly with increasing irradiation intensity up to 1 sun, suggesting that the photocurrent is not limited by the bimolecular recombination under the short-circuit condition.[8] On the other hand, the open-circuit voltage has been reported to be primarily limited by bimolecular recombination.[9] In other words, the impact of the bimolecular recombination on the device performance is not fully understood.

The bimolecular recombination in blend films, including P3HT:PCBM, has been studied by transient absorption spectroscopy,[9−13] photogenerated charge carrier extraction by linearly increasing voltage technique (photo-CELIV),[14,15] and time-of-flight measurements.[16,17] Recent studies have also shown that the bimolecular recombination rate in P3HT:PCBM blend films

[†] Kyoto University.
[‡] JST PRESTO.

(1) Günes, S.; Neugebauer, H.; Sariciftci, N. S. *Chem. Rev.* **2007**, *107*, 1324–1338.
(2) Brabec, C. J.; Durrant, J. R. *MRS Bull.* **2008**, *33*, 670–675.
(3) Thompson, B. C.; Fréchet, J. M. J. *Angew. Chem., Int. Ed.* **2008**, *47*, 58–77.
(4) Ma, W.; Yang, C.; Gong, X.; Lee, K.; Heeger, A. J. *Adv. Funct. Mater.* **2005**, *15*, 1617–1622.
(5) Li, G.; Shrotriya, V.; Huang, J.; Yao, Y.; Moriarty, T.; Emery, K.; Yang, Y. *Nat. Mater.* **2005**, *4*, 864–868.
(6) Kim, Y.; Cook, S.; Tuladhar, S. M.; Choulis, S. A.; Nelson, J.; Durrant, J. R.; Bradley, D. D. C.; Giles, M.; McCulloch, I.; Ha, C.-S.; Ree, M. *Nat. Mater.* **2006**, *5*, 197–203.
(7) Honda, S.; Nogami, T.; Ohkita, H.; Benten, H.; Ito, S. *ACS Appl. Mater. Interfaces* **2009**, *1*, 804–810.
(8) Schilinsky, P.; Waldauf, C.; Brabec, C. J. *Appl. Phys. Lett.* **2002**, *81*, 3885–3887.
(9) Shuttle, C. G.; O'Regan, B.; Ballantyne, A. M.; Nelson, J.; Bradley, D. D. C.; Durrant, J. R. *Phys. Rev. B* **2008**, *78*, 113201.
(10) Clarke, T. M.; Jamieson, F. C.; Durrant, J. R. *J. Phys. Chem. C* **2009**, *113*, 20934–20941.
(11) Montanari, I.; Nogueira, A. F.; Nelson, J.; Durrant, J. R.; Winder, C.; Loi, M. A.; Sariciftci, N. S.; Brabec, C. *Appl. Phys. Lett.* **2002**, *81*, 3001–3003.
(12) Nogueira, A. F.; Montanari, I.; Nelson, J.; Durrant, J. R.; Winder, C.; Sariciftci, N. S.; Brabec, C. *J. Phys. Chem. B* **2003**, *107*, 1567–1573.
(13) Nelson, J. *Phys. Rev. B* **2003**, *67*, 155209.
(14) Foertig, A.; Baumann, A.; Rauh, D.; Dyakonov, V.; Deibel, C. *Appl. Phys. Lett.* **2009**, *95*, 052104.
(15) Juška, G.; Genevičius, K.; Nekrašas, N.; Sliaužys, G.; Dennler, G. *Appl. Phys. Lett.* **2008**, *93*, 143303.
(16) Pivrikas, A.; Juška, G.; Mozer, A. J.; Scharber, M.; Arlauskas, K.; Sariciftci, N. S.; Stubb, H.; Österbacka, R. *Phys. Rev. Lett.* **2005**, *94*, 176806.
(17) Sliaužys, G.; Juška, G.; Arlauskas, K.; Pivrikas, A.; Österbacka, R.; Scharber, M.; Mozer, A.; Sariciftci, N. S. *Thin Solid Films* **2006**, *511−512*, 224–227.

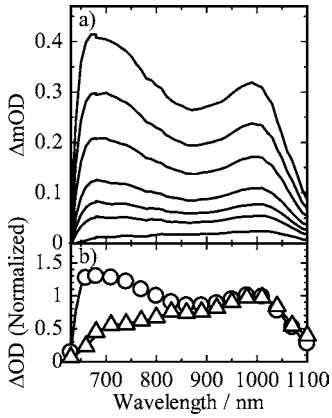

Figure 1. Microsecond transient absorption spectra of P3HT:PCBM blend films excited at 400 nm (30 μJ cm^{-2}) measured at a) 0.5, 1, 2, 5, 10, 20, and 100 μs from top to bottom, and the transient absorption spectra normalized at 1000 nm measured at 0.5 (○) and 100 μs (△).

is orders of magnitude slower than the Langevin recombination rate, $\gamma_L = e(\mu_e + \mu_h)/\varepsilon\varepsilon_0$, suggesting that the bimolecular recombination does not lead to an actual loss in this solar cell.[9,16] Furthermore, the recombination dynamics also has been discussed in terms of the bimolecular recombination rate depending on time or charge density: apparently such time-dependent bimolecular recombination rate results in trimolecular recombination kinetics.[9,14,15,18,19] The time-dependent bimolecular recombination rate is explained in connection with the recombination in disordered polymer solids with an exponential tail of trapped polarons.[10,12,13] In other words, the bimolecular recombination dynamics in such blend films is considered to be limited by multiple trapping and detrapping, which would cause trap-limited charge transport in P3HT:PCBM solar cells. Nonetheless, as mentioned above, P3HT:PCBM solar cells exhibit relatively high fill factors and EQEs, indicating that the device performance is not limited by the charge transport.

On the other hand, the charge transport in P3HT pristine films have been studied in field-effect transistor (FET) configuration.[20] The FET hole mobility in P3HT pristine films has been reported to be as high as 0.1 cm^2 V^{-1} s^{-1}, observed for the P3HT film with higher regioregularity, suggesting that the high hole mobility is closely related to the crystallization of P3HT. Recently, charge modulation spectroscopy of P3HT-based FET has revealed two kinds of polarons in P3HT pristine films:[21,22] "interchain delocalized polarons" and "intrachain localized polarons". The formation ratio of the two polarons is dependent on the film morphology.[20] A higher fraction of "interchain delocalized polarons" is observed for P3HT films with higher regioregularity and hole mobility, suggesting that "interchain delocalized polarons" play a major role in efficient hole transport in P3HT pristine films. In contrast, little is known about the major charge carrier in P3HT:PCBM blend films, which is essential for developing highly efficient polymer solar cells.

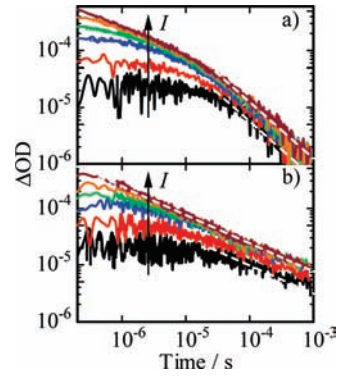

Figure 2. Microsecond transient absorption decays of P3HT:PCBM blend films measured at (a) 700 nm and (b) 1000 nm. The excitation intensity was varied over 0.8, 1.8, 4.7, 7.4, 14, and 30 μJ cm^{-2} from bottom to top in each panel. The transient absorption decays were fitted with a power-law function of $\Delta OD \propto t^{-\alpha}$. The broken lines represent the best fitting curves with $\alpha \approx 1$ for the 700-nm band and $\alpha \approx 0.5$ for the 1000-nm band.

Herein we report the existence of two polarons even in P3HT:PCBM blend films as in P3HT pristine films as mentioned above and quantitatively analyze the different bimolecular recombination dynamics of the two polarons by transient absorption spectroscopy at various excitation intensities and temperatures. The delocalized polarons exhibit a trap-free bimolecular recombination dynamics, while the localized polarons exhibit a trap-limited bimolecular recombination dynamics. Furthermore, we demonstrate that the localized polarons have a trap-depth profile that consists of a Gaussian distribution and an exponential tail as predicted theoretically. On the basis of these quantitative analyses, we discuss the relevance of the bimodal polarons and charge transport to the device performance of polymer solar cells.

2. Results

2.1. Transient Absorption Spectra. Figure 1a shows the transient absorption spectra of a P3HT:PCBM blend film measured from 0.5 to 100 μs after the laser excitation at 400 nm with a fluence of 30 μJ cm^{-2}. Two absorption bands were clearly observed at around 700 and 1000 nm. Interestingly, the 700-nm band decayed faster than the 1000-nm band. Figure 1b shows the transient absorption spectra at 0.5 and 100 μs that are normalized at 1000 nm. As shown in this figure, the 700-nm band almost disappeared and the 1000-nm band was dominant at 100 μs. Both bands decayed on a microsecond time scale, which is too long to be assigned to singlet excitons. No change in the decay dynamics was observed for both bands under an O_2 atmosphere. In other words, these bands are assigned to neither singlet excitons nor triplet excitons. We therefore assign these two bands to different charged species as discuss later.

2.2. Transient Absorption Decay. To address the origin of the different decay dynamics in the P3HT:PCBM blend film, we measured transient absorption decays at 700 and 1000 nm at different excitation intensities from 0.8 to 30 μJ cm^{-2}. We first focus our attention on a time scale shorter than 10 μs. As shown in Figure 2, both bands decayed faster with increasing excitation intensity, indicating the decay dynamics due to bimolecular recombination of charged carriers. Furthermore, they exhibited the same decay dynamics at the same excitation

(18) Shuttle, C. G.; O'Regan, B.; Ballantyne, A. M.; Nelson, J.; Bradley, D. D. C.; de Mello, J.; Durrant, J. R. *Appl. Phys. Lett.* **2008**, *92*, 093311.
(19) Shuttle, C. G.; Maurano, A.; Hamilton, R.; O'Regan, B.; de Mello, J. C.; Durrant, J. R. *Appl. Phys. Lett.* **2008**, *93*, 183501.
(20) Sirringhaus, H.; Brown, P. J.; Friend, R. H.; Nielsen, M. M.; Bechgaard, K.; Langeveld-Voss, B. M. W.; Spiering, A. J. H.; Janssen, R. A. J.; Meijer, E. W.; Herwig, P.; de Leeuw, D. M. *Nature* **1999**, *401*, 685–688.
(21) Österbacka, R.; An, C. P.; Jiang, X. M.; Vardeny, Z. V. *Science* **2000**, *287*, 839–842.
(22) Jiang, X.; Österbacka, R.; Korovyanko, O.; An, C. P.; Horovitz, B.; Janssen, R. A. J.; Vardeny, Z. V. *Adv. Funct. Mater.* **2002**, *12*, 587–597.

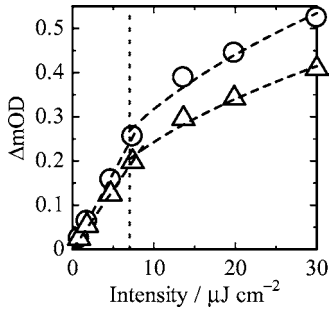

Figure 3. Intensity dependence of the transient signals at 700 nm (○) and 1000 nm (△) of P3HT:PCBM blend films measured at 0.2 μs. The broken lines represent fitting curves. The dotted line exhibits a turning point from linear to sublinear dependence of the transient signals (~7 μJ cm^{-2}).

intensity, suggesting that these different charged species are subject to the same bimolecular recombination dynamics on this short time scale. Figure 3 shows the transient absorption signals at 0.2 μs of the 700-nm band (○) and the 1000-nm band (△) at excitation intensities ranging from 0.8 to 30 μJ cm^{-2}. Both signals increased linearly with increasing excitation intensity at intensities <7 μJ cm^{-2}, and increased sublinearly at intensities >7 μJ cm^{-2}. The sublinear intensity dependence suggests that the bimolecular recombination is already dominant on a time scale shorter than 0.2 μs because of higher carrier densities. We note that the two bands exhibit the same intensity dependence including a turning point of 7 μJ cm^{-2} from linear to sublinear region. This result also suggests that these different charged species observed at 700 and 1000 nm obey the same bimolecular recombination dynamics on a time scale shorter than 10 μs.

In contrast, the decay dynamics were different on a time scale longer than 10 μs as shown in Figure 2. Both transient absorption decays can be fitted by a power-law function of $\Delta OD \propto t^{-\alpha}$ with a different exponent α. The exponent for the 1000-nm decay was ~0.5, which is consistent with previous reports.[6,9,10,23] This power-law decay with an exponent $\alpha < 1$ is characteristic of bimolecular recombination of trapped carriers having an exponential tail of polaron trap states (trap-limited bimolecular recombination).[10–13] Interestingly, the exponent (α) for the 700-nm band was as high as 1. The possible mechanisms for the power-law decay with $\alpha \approx 1$ are trap-free bimolecular recombination or multistep tunneling recombination of trapped carriers.[13] We will discuss the mechanism later. Note that the exponents (α) before the thermal annealing were ~0.4 for the 1000-nm band and ~0.7 for the 700-nm band (see the Supporting Information) while amorphous blend films of regiorandom P3HT and PCBM exhibited an exponent of 0.35.[24] This result suggests that the recombination dynamics is strongly dependent on the film morphology.

2.3. Temperature Dependence. To elucidate the mechanism of the charge recombination dynamics in the P3HT:PCBM blend film, we measured the transient absorption decay monitored at 700 and 1000 nm at different temperatures from 150 to 290 K. As shown in Figure 4, both bands decayed more slowly with decreasing temperature, suggesting a smaller bimolecular recombination rate at lower temperatures.[14] In other words, the

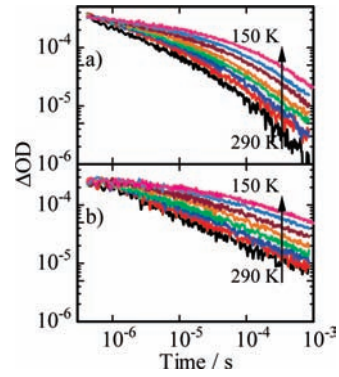

Figure 4. Microsecond transient absorption decays of P3HT:PCBM blend films excited at 14 μJ cm^{-2} measured at (a) 700 nm and (b) 1000 nm. The measurement temperature was varied over 290, 270, 250, 230, 210, 190, 170, and 150 K from bottom to top in each panel.

recombination both at 700 and 1000 nm is a thermally activated process. This is consistent with the trap-limited bimolecular recombination, which is the 1000-nm decay dynamics we assigned. On the other hand, it is inconsistent with multistep tunneling recombination of trapped carriers, which has been reported to be independent of temperature.[13,25–27] We therefore ascribe the decay dynamics observed at 700 nm to the thermally activated trap-free bimolecular recombination rather than the multistep tunneling recombination, and the decay at 1000 nm to the trap-limited bimolecular recombination.

3. Discussion

3.1. Assignments. We first summarize the assignments of transient species observed for P3HT:PCBM blend films on a microsecond time scale before discussing the bimolecular recombination in detail. As mentioned above, the absorption bands at 700 and 1000 nm can be ascribed neither to singlet excitons nor to triplet excitons but rather to charged species. Furthermore, the PCBM anion has an absorption band at 1020 nm with a molar absorption coefficient of 6.0×10^3 M^{-1} cm^{-1},[28] which is approximately 1 order of magnitude smaller than P3HT polarons as mentioned below. In other words, these bands can be basically ascribed to P3HT polarons. Previously, we have assigned these bands to dissociated polarons because the decay dynamics depended on the excitation intensity.[24] Considering the difference in the exponents (α) mentioned above, we attributed the decay dynamics of the 700-nm band to trap-free bimolecular recombination and the decay dynamics of the 1000-nm band to trap-free bimolecular recombination on shorter time scales (<10 μs) and to trap-limited bimolecular recombination on longer time scales (>10 μs). We therefore assign the 700-nm band to polarons in crystalline P3HT domains and the 1000-nm band to polarons in relatively disordered (amorphous-like) P3HT domains, which would be interfacial area between crystalline P3HT domains and aggregates of PCBM nanocrystals.[29,30] The assignment for the 1000-nm band is consistent with previous

(23) Ohkita, H.; Cook, S.; Astuti, Y.; Duffy, W.; Tierney, S.; Zhang, W.; Heeney, M.; McCulloch, I.; Nelson, J.; Bradley, D. D. C.; Durrant, J. R. *J. Am. Chem. Soc.* **2008**, *130*, 3030–3042.
(24) Guo, J.; Ohkita, H.; Benten, H.; Ito, S. *J. Am. Chem. Soc.* **2010**, *132*, 6154–6164.
(25) Marumoto, K.; Muramatsu, Y.; Kuroda, S. *Appl. Phys. Lett.* **2004**, *84*, 1317–1319.
(26) Chwang, A. B.; Frisbieb, C. D. *J. Appl. Phys.* **2001**, *90*, 1342–1349.
(27) Ohkita, H.; Sakai, W.; Tsuchida, A.; Yamamoto, M. *Bull. Chem. Soc. Jpn.* **1997**, *70*, 2665–2670.
(28) Yamamoto, S.; Guo, J.; Ohkita, H.; Ito, S. *Adv. Funct. Mater.* **2008**, *18*, 2555–2562.
(29) Yang, X.; Loos, J.; Veenstra, S. C.; Verhees, W. J. H.; Wienk, M. M.; Kroon, J. M.; Michels, M. A. J.; Janssen, R. A. J. *Nano Lett.* **2005**, *5*, 579–583.

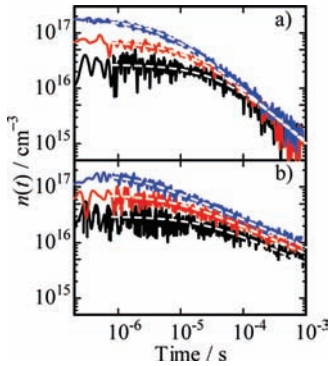

Figure 5. Carrier density decays of P3HT:PCBM blend films measured at (a) 700 nm and (b) 1000 nm excited at 0.8, 1.8, and 4.7 μJ cm^{-2} from bottom to top in each panel. The broken lines represent fitting curves with an empirical power equation: $n(t) = n_0(1 + at)^{-\alpha}$.

transient absorption studies.[23,31] On the other hand, the 700-nm band has not been observed in transient absorption studies of P3HT:PCBM blends on a microsecond time scale. This band is consistent with two-dimensionally delocalized polarons assigned by charge modulation spectroscopy of P3HT-based FET in the accumulation regime[20] and also photoinduced absorption spectroscopy of P3HT pristine films.[21,22] In these previous studies on P3HT pristine films, the 700- and 1000-nm bands are ascribed to interchain delocalized polarons and intrachain localized polarons, respectively. This assignment is consistent with our observation of two different recombination dynamics in P3HT:PCBM blends: trap-free bimolecular recombination for the 700-nm band and trap-limited bimolecular recombination for the 1000-nm band. Note that both the delocalized polarons and the localized polarons can be formed on a time scale of less than nanoseconds.[24]

3.2. Bimodal Recombination. Here we analyze the transient absorption dynamics at 700 and 1000 nm at modest excitation intensities of <1.8 μJ cm^{-2} because, as mentioned below, the carrier density at 1.8 μJ cm^{-2} is comparable to that under the solar irradiation of 1 sun ($\sim 10^{17}$ cm^{-3}).[18] For the quantitative discussion, the transient absorption signal ΔOD(t) should be converted into the carrier density $n(t)$. According to the Beer−Lambert law, the carrier density is directly related to the transient absorption decay as follows:

$$n(t) = \Delta\mathrm{OD}(t) N_\mathrm{A} (1000 \varepsilon l)^{-1} \quad (1)$$

where ΔOD(t) is the transient absorption signal measured at a delay time t, N_A is the Avogadro's constant (6.02×10^{23} mol^{-1}), ε is the molar absorption coefficient of polarons (3.5×10^4 M^{-1} cm^{-1} at 700 nm and 3.0×10^4 M^{-1} cm^{-1} at 1000 nm, see the Supporting Information), and l is the thickness of the blend film (160 nm). Figure 5 shows the time evolution of the carrier density of delocalized polarons observed at 700 nm and localized polarons observed at 1000 nm, which are converted by eq 1 from Figure 2. Both bands were well fitted with the following empirical power equation.

$$n(t) = n_0(1 + at)^{-\alpha} \quad (2)$$

As shown in Figure 5, α is equal to unity for the delocalized polaron band at 700 nm and $\sim$0.5 for the localized polaron band at 1000 nm. The difference in α suggests the different recombination dynamics of these two polarons as discussed below.

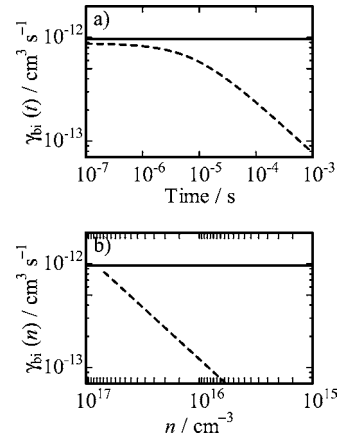

Figure 6. Plots of the bimolecular recombination rate γ_{bi} at 700 nm (solid lines) and 1000 nm (broken lines) (a) as a function of time t and (b) as a function of the carrier density n.

In the diffusion-limited bimolecular charge recombination, the decay of carrier density is given by

$$\mathrm{d}n(t)/\mathrm{d}t = -\gamma_{bi}(t) n^2(t) \quad (3)$$

where $n(t)$ is the carrier density and $\gamma_{bi}(t)$ is the bimolecular recombination rate at a delay time t. Therefore, the time-dependent bimolecular recombination rate can be obtained by combining eqs 2 and 3, which can be also expressed as a function of the carrier density by combining eqs 2 and 4.

$$\gamma_{bi}(t) = -\mathrm{d}n(t)/\mathrm{d}t n^{-2}(t) = a\alpha n_0^{-1}(1 + at)^{\alpha - 1} \quad (4)$$

$$\gamma_{bi}(n) = a\alpha n_0^{-1/\alpha} n^{(1/\alpha)-1} \quad (5)$$

As mentioned above, α is equal to unity for the delocalized polaron band at 700 nm and $\sim$0.5 for the localized polaron band at 1000 nm. Therefore, as shown in Figure 6, the bimolecular recombination rate is time-independent $\gamma_{bi} = an_0^{-1} \approx 10^{-12}$ cm^3 s^{-1} for the delocalized polaron band at 700 nm, and time-dependent $\gamma_{bi}(t)$ for the localized polaron band at 1000 nm, which decreases from 10^{-12} to 10^{-13} cm^3 s^{-1} over the time range from 10^{-6} to 10^{-3} s.

The time-independent trap-free bimolecular recombination rate $\gamma_{bi} \approx 10^{-12}$ cm^3 s^{-1} is 1 order of magnitude higher than that estimated by photo-CELIV.[16] This is probably because the photo-CELIV measurement cannot distinguish these two charged carriers and hence gives the averaged bimolecular recombination rate. Interestingly, even the trap-free bimolecular recombination rate is still 2 orders of magnitude lower than the Langevin recombination rate given by $\gamma_L = e(\mu_e + \mu_h)/\varepsilon\varepsilon_0 \approx 10^{-10}$ cm^3 s^{-1} with $\mu_e \approx \mu_h \approx 10^{-4}$ cm^3 V^{-1} s^{-1}.[32] As reported previously, the reduced bimolecular recombination rate is ascribed to phase-separated bicontinuous network of P3HT and PCBM domains, which is beneficial for reducing bimolecular recombination loss.[9,16] More importantly, the lifetime of trap-free carriers is estimated to be $\tau = (\gamma_{bi} n_0)^{-1} \approx 10$ μs under the 1 sun condition, which is comparable to a charge collection time to extract $\sim$70% charges under the 1 sun open-circuit conditions.[19] This finding suggests that a majority of trap-free charge carriers can reach the electrode without bimolecular recombination even under the

(30) van Bavel, S. S.; Sourty, E.; de With, G.; Loos, J. *Nano Lett.* **2009**, *9*, 507–513.
(31) Clarke, T. M.; Ballantyne, A. M.; Nelson, J.; Bradley, D. D. C.; Durrant, J. R. *Adv. Funct. Mater.* **2008**, *18*, 4029–4035.
(32) Baumann, A.; Lorrmann, J.; Deibel, C.; Dyakonov, V. *Appl. Phys. Lett.* **2008**, *93*, 252104.

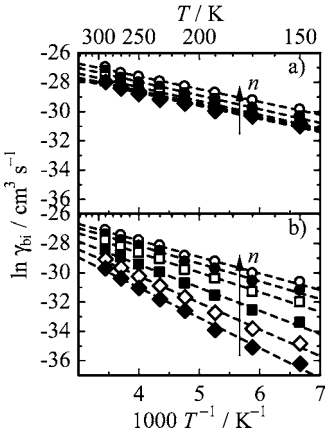

Figure 7. Arrhenius plots of the bimolecular recombination rate γ_{bi} at (a) 700 nm and (b) 1000 nm against the temperature from 150 to 290 K. The carrier densities (n) were varied over 1.3×10^{16} (♦), 2.7×10^{16} (◇), 5.4×10^{16} (■), 1.1×10^{17} (□), 1.6×10^{17} (●), 2.2×10^{17} cm^{-3} (○) at 700 nm and varied over 1.3×10^{16} (♦), 2.5×10^{16} (◇), 5.0×10^{16} (■), 1.0×10^{17} (□), 1.5×10^{17} (●), 2.0×10^{17} cm^{-3} (○) at 1000 nm from bottom to top. The broken lines represent fitting curves with the Arrhenius equation: $\ln \gamma_{bi} = \ln A - E_A/(k_B T)$.

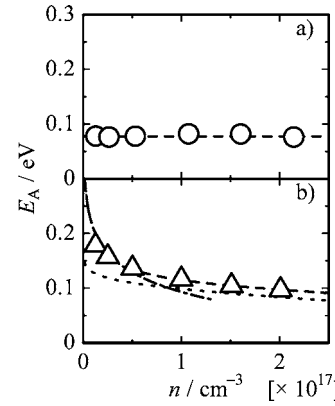

Figure 8. Plots of the activation energy E_A at (a) 700 nm (○) and (b) 1000 nm (△) against the carrier density. The plots at 700 nm were fitted with a constant: $E_A = B$. The plots at 1000 nm were fitted with the following functions: $n = N_1 \exp[(E - E_0)/(k_B T_0)] + 0.5N_2/[(2\pi)^{0.5}\,\sigma)]\,\{1 + \mathrm{erf}[(E - E_0)/(2^{0.5}\,\sigma)]\}$, where erf($x$) is the error function indicating the integral of Gaussian function. The broken lines represent the best fitting curves. The dashed−dotted and dotted lines indicate the integrals of exponential and Gaussian functions, respectively.

open-circuit condition. We note that before the thermal annealing only ~40% of charges can survive even at the same collection time of ~10 μs under the 1 sun open-circuit conditions (see Figure S4, Supporting Information). In other words, the recombination loss under the open-circuit condition is strongly dependent on the film morphology as we have reported recently.[24] Under the short-circuit condition, as mentioned before, the recombination loss has been reported to be negligible because the short-circuit current increases linearly with the illumination intensity. We therefore conclude that trap-free polarons play a major role in the charge transport, resulting in the recombination-lossless performance in P3HT:PCBM solar cells under not only the short-circuit but also the open-circuit condition. This is consistent with the relatively high fill factors (0.6−0.7) and EQEs (>80%) reported for this device compared to other combination devices.[4–7]

On the other hand, the time-dependent trap-limited bimolecular recombination rate $\gamma_{bi}(t)$ varies from 10^{-12} to 10^{-13} cm^3 s^{-1} depending on time or carrier density, as shown in Figure 6, which is consistent with previous reports.[9,14] The origin of the time-dependent bimolecular recombination rate is explained by bimolecular recombination of trapped carriers whose trap depths depend on the carrier density: the trap depth deepens with time because of lower carrier density, resulting in the slower bimolecular recombination rate on longer time scales.[10,12,13] We should note the relationship between the time-dependent bimolecular recombination rate and trimolecular recombination dynamics reported for P3HT:PCBM blends recently.[9,14,15] As shown in Figure 6b, the slope of log−log plots of $\gamma_{bi}(n)$ against n is almost unity and therefore $\gamma_{bi}(n)$ can be expressed by $\gamma_{bi}(n) \approx \gamma_0\, n$. Consequently, eq 3 is rewritten by

$$\mathrm{d}n(t)/\mathrm{d}t \approx -\gamma_0 n^3(t) \qquad (6)$$

More specifically, $\gamma_{bi}(n)$ can be expressed by eq 5 ($\gamma_{bi}(n) \propto n^{(1/\alpha)-1}$) and α varies over 0.37−0.5 for localized polarons at 1000 nm in the P3HT:PCBM blend films before and after the thermal annealing (see the Supporting Information), and is reported to be around 0.3−0.7 for polarons in other P3HT:PCBM blends with different PCBM fractions or under different annealing conditions.[6,9,10,23] Therefore, the exponent in eq 6 would vary from 4.3 to 2.4 depending on such variations in α from 0.3 to 0.7. In other words, the time-dependent trap-limited bimolecular recombination rate is strongly dependent on the film morphology. This would be related to hole transfer from amorphous to crystalline domains. Indeed, we have recently reported such hole transfer from amorphous to crystalline domains in P3HT:PCBM blends on a time scale of subnanoseconds.[24] Considering the difference in ionization potential, hole polarons are likely to transfer to crystalline domains because the amorphous P3HT has a higher ionization potential than the crystalline P3HT.[31,33]

3.3. Trap Depth Profile. To evaluate the trap depth quantitatively, we analyzed the transient absorption dynamics at 700 and 1000 nm, measured at different temperatures and carrier densities, in the same way described above. Figure 7 shows temperature dependence of the bimolecular recombination rate of (a) delocalized polarons observed at 700 nm and (b) localized polarons at 1000 nm over the carrier density range from 10^{16} to 10^{17} cm^{-3}. For the delocalized polarons, the activation energy estimated from the slope in the Arrhenius plot is ~0.078 eV independently of the carrier density, which is comparable to the activation energy for the mobility of P3HT pristine films evaluated in FET configuration (0.08−0.1 eV).[20] On the other hand, the activation energy for the localized polarons varies from 0.097 to 0.178 eV depending on the carrier density, which is rather comparable to the activation energy for the mobility of P3HT pristine films evaluated from the space-charge limited current (SCLC) (~0.13 eV).[34] The carrier density is typically >10^{18} cm^{-3} in FET and ~10^{16} cm^{-3} in SCLC measurements.[35] In other words, trap-free charge transport is dominant under the FET operation condition because of trap filling, while trap-limited charge transport is dominant in the SCLC measurement because of incomplete trap filling. Therefore, the agreement in the activation energy is also consistent with our bimolecular recombination analysis described above.

Figure 8 shows the dependence of the activation energy on

(33) Stevens, D. M.; Qin, Y.; Hillmyer, M. A.; Frisbie, C. D. *J. Phys. Chem. C* **2009**, *113*, 11408–11415.
(34) Goh, C.; Kline, R. J.; McGehee, M. D.; Kadnikova, E. N.; Fréchet, J. M. J. *Appl. Phys. Lett.* **2005**, *86*, 122110.
(35) Mihailetchi, V. D.; Koster, L. J. A.; Hummelen, J. C.; Blom, P. W. M. *Phys. Rev. Lett.* **2004**, *93*, 216601.

Scheme 1. Schematic Illustration of Phase-Separated Structures and Bimodal Hole Transport in P3HT:PCBM Blend Films.[a]

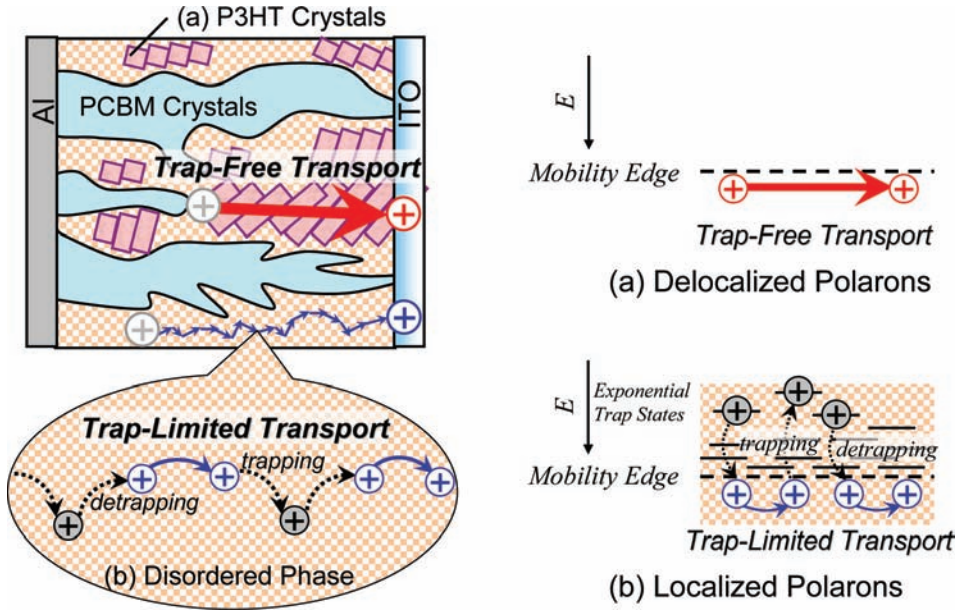

[a] Phase-separated structures consisting of fibrillar networks of P3HT nanocrystals, disordered P3HT matrices including PCBM nanocrystals, and aggregates of PCBM nanocrystals are formed in P3HT:PCBM blend films after thermal annealing. The delocalized polarons formed in fibrillar networks of P3HT nanocrystals exhibit a trap-free hole transport. On the other hand, the localized polarons formed in disordered P3HT domains exhibit a trap-limited hole transport due to multiple trapping and detrapping. The right side in this figure shows the relative energy levels for each hole transport.

the carrier density evaluated from the Arrhenius plots. As mentioned above, the activation energy for the delocalized polarons is independent of the carrier density (Figure 8a). This energy is comparable to that evaluated in FET configuration but smaller than that (~0.025 eV) evaluated by time-resolved microwave photoconductivity, which is sensitive to the carrier motion in a grain boundary because of the high frequency of the electric field (>GHz).[36] Therefore, the activation energy we observed is ascribed to the energy that delocalized polarons in a charge transport state require for the charge hopping between grain boundaries. On the other hand, the activation energy for the localized carriers decreases with the increase in the carrier density (Figure 8b). Therefore, this energy is ascribed to the energy that localized polarons require to escape from trap sites to the charge transport state. We speculate that this transport state is similar in energy to that for delocalized polarons because the bimolecular recombination rate is almost the same at higher carrier densities. Therefore, this profile represents the energetic distribution of trap density for the localized polarons. Interestingly, the energetic distribution can be fitted with the integral expression of the density of states described by a sum of exponential and Gaussian functions in eq 7, as theoretically predicted,[11–13,37]

$$n = N_1\exp[(E - E_0)/(k_BT_0)] + 0.5N_2/[(2\pi)^{0.5}\sigma)]\{1 + \mathrm{erf}[(E - E_0)/(2^{0.5}\sigma)]\} \quad (7)$$

where N_1 is the integrated polaron densities in the exponential tail, E is the trap-depth energy at the carrier density n, which is equal to $-E_A$, E_0 is the energy for charge hopping in the charge transport state (−0.078 eV), k_B is the Boltzmann constant, T_0 represents the distribution of polaron trap states, which was evaluated to be 596 K from the power-law decay with $\alpha \approx 0.5$ at room temperature by the following relation: $\alpha = T/T_0$,[13] N_2 is the integrated polaron densities in the Gaussian distribution, and σ is the standard deviation of the Gaussian distribution.

From the fitting, the standard deviation σ is estimated to be 0.025 eV, which is comparable to k_BT at room temperature, suggesting that localized polarons in the Gaussian distribution can freely migrate as trap-free carriers at the mobility edge. Recent Monte Carlo simulations of carrier mobility in organic solids have also shown that the carrier mobility is independent of the carrier density when the half width σ is as small as k_BT at room temperature.[38,39] This is consistent with our observation of trap-free bimolecular recombination for the 1000-nm band at higher excitation intensities: even localized polarons can freely migrate as trap-free carriers at higher carrier densities. As shown in Figure 8, some of the localized polarons are located in the Gaussian distribution at $\sim 10^{17}$ cm^{-3} corresponding to the 1 sun open-circuit condition. Therefore, we conclude that not only delocalized polarons but also some of the localized polarons can contribute to the hole transport under the 1 sun open-circuit condition. Recent studies have shown that there are three phases in P3HT:PCBM blends: fibrillar network of P3HT crystals, aggregates of PCBM nanocrystals, and relatively disordered P3HT matrices with PCBM nanocrystals.[29,30] We therefore speculate, as illustrated in Scheme 1, that delocalized polarons formed in the fibrillar network of P3HT crystals exhibit trap-free bimolecular recombination dynamics and hence can migrate freely, while localized polarons formed in disordered P3HT matrices exhibit trap-limited bimolecular recombination dynamics due to multiple trapping and detrapping. Under the 1 sun illumination, even the localized polarons can also migrate freely in disordered P3HT matrices because some trap sites are filled

(36) Dicker, G.; de Haas, M. P.; Siebbeles, L. D. A.; Warman, J. M. *Phys. Rev. B* **2004**, *70*, 045203.
(37) Westerling, M.; Österbacka, R.; Stubb, H. *Phys. Rev. B* **2002**, *66*, 165220.
(38) Zhou, J.; Zhou, Y. C.; Zhao, J. M.; Wu, C. Q.; Ding, X. M.; Hou, X. Y. *Phys. Rev. B* **2007**, *75*, 153201.
(39) Pasveer, W. F.; Cottaar, J.; Tanase, C.; Coehoorn, R.; Bobbert, P. A.; Blom, P. W. M.; de Leeuw, D. M.; Michels, M. A. J. *Phys. Rev. Lett.* **2005**, *94*, 206601.

with excess polarons. In other words, such trap fillings can improve the total hole mobility, resulting in a better balance of hole and electron transport[40] and further leading to high fill factor and EQE, because the electron mobility is typically higher than the hole mobility in P3HT:PCBM blend films.[41] On the other hand, the thermal annealing can also improve the charge transport: the exponents (α) of the power-law decays for both delocalized polarons and localized polarons increase remarkably after the thermal annealing (see Figure S5, Supporting Information). These findings are consistent with our recent report that the charge collection efficiency is drastically improved by the thermal annealing.[24] We thus conclude that the efficient bimodal hole transport plays a key role in relatively high fill factors and EQEs observed for P3HT:PCBM solar cells.

4. Conclusions

We have studied the bimolecular recombination dynamics for P3HT:PCBM blend films by transient absorption spectroscopy at various excitation intensities and temperatures. We observed two characteristic transient absorption bands of P3HT polarons at 700 and 1000 nm, which are ascribed to delocalized polarons formed in fibrillar networks of P3HT crystals and to localized polarons in relatively disordered P3HT matrices, respectively. The delocalized polarons decayed with a time-independent bimolecular recombination rate of $\sim 10^{-12}$ cm^3 s^{-1} independently of the carrier density. The activation energy for the bimolecular recombination of delocalized polarons was independent of the carrier density and was as small as $\sim$0.078 eV, which is ascribed to the energy required for the charge hopping between grain boundaries in P3HT crystalline domains. On the other hand, the localized polarons decayed with a time-dependent bimolecular recombination rate. The recombination rate depends on the charge density and approaches 10^{-12} cm^3 s^{-1} which is comparable to that of delocalized polarons at higher charge densities $\sim 10^{17}$ cm^{-3}. The activation energy for the bimolecular recombination of localized polarons decreased from 0.178 to 0.097 eV with increasing carrier density from 1×10^{16} to 2×10^{17} cm^{-3}, which is ascribed to the energy required for trapped polarons to escape to a charge transport state in disordered P3HT domains. The trap depth profile can be fitted with the integral expression of the density of states described by a sum of Gaussian distribution and an exponential tail, which is fully consistent with a theoretical model proposed by Nelson. We therefore conclude that delocalized polarons play a primary role in trap-free charge transport in P3HT:PCBM blend films and some of localized polarons also contribute to the trap-free charge transport under the 1 sun condition although they cause a trap-limited charge transport in disordered P3HT domains at lower carrier densities. More importantly, the lifetime of such trap-free polarons is estimated to be $\sim$10 μs under the 1 sun condition, which is comparable to the charge collection time to extract $\sim$70% charges under the 1 sun open-circuit condition, suggesting that trap-free polarons play a key role in the recombination-lossless charge transport in P3HT:PCBM solar cells under not only the short-circuit but also the open-circuit condition. The bimodal charge transport based on two polarons with different delocalization may substantially contribute to the relatively high fill factors and EQEs of P3HT:PCBM solar cells. Our findings are closely related to self-assembled P3HT networks, which will help in designing polymer solar cells with higher fill factors and EQEs.

5. Experimental Section

Sample Preparation. Blend films of regioregular poly(3-hexylthiophene) (P3HT, Aldrich, head-to-tail >98%, $M_w = 50300$, $M_w/M_n = 2.2$) and [6,6]-phenyl-C_{61}-butyric acid methyl ester (PCBM, Frontier Carbon, >99%) were prepared onto quartz substrates by spin-coating from a chlorobenzene (Aldrich) solution of P3HT and PCBM (1:1 by weight) at a concentration of $\sim$20 mg mL^{-1}. Before the spin-coating, the blend solution was stirred at 40 °C overnight. The P3HT:PCBM blend film was thermally annealed at 140 °C for 30 min. The film thickness was approximately 160 nm. The substrates employed were cleaned by ultrasonic treatment in toluene, acetone, and ethanol for 15 min.

Measurements. Transient absorption data were collected with a highly sensitive microsecond transient absorption system.[28] In the microsecond transient absorption measurement, a dye laser (Photon Technology International Inc., GL-301) pumped by a nitrogen laser (Photon Technology International Inc., GL-3300) was used as an excitation source, which provides subnanosecond pulses with various fluences from $\sim\mu$J to 0.1 mJ cm^{-2} at a repetition rate of 4 Hz. The excitation wavelength was 400 nm. A tungsten lamp (Thermo-Oriel, model 66997) with an intensity controller (Thermo-Oriel, model 66950) was used as a probe light source. The probe wavelength was selected by two monochromators (Ritsu, MC-10C) and appropriate optical cutoff filters equipped before and after the sample to reduce scattered light and emission. The temporal evolution of ΔOD was recorded using a high-gain Si photodiode (Hamamatsu Photonics, S1722-01). The signal from the photodiode was preamplified and sent to a main amplifier (Costronics Electronics) with an electronic band-pass filter to improve the signal-to-noise ratio. Finally, the amplified signal was collected using a digital oscilloscope (Tektronix, TDS2022), which was synchronized with a trigger signal of the laser pulse from a Si photodiode (Thorlabs Inc., DET10A). The instrument response was of the order of 60 ns. Transient absorption decays were collected over the time range from submicroseconds to milliseconds, averaging 400 laser shots on each delay time scale, yielding a sensitivity of 10^{-6} to 10^{-4}, depending on the measuring time domain. The sample film was sealed in a quartz cuvette purged with Ar for 30 min for room-temperature measurement, and set in a cryostat chamber (Iwatani Plantech Corp., CRT510) with a PID temperature control unit (Scientific Instruments, model 9650) for temperature-dependence measurements.

Acknowledgment. This work was supported by the JST PRESTO program and the Global COE program (International Center for Integrated Research and Advanced Education in Materials Science) from the Ministry of Education, Culture, Sports, Science, and Technology, Japan.

Supporting Information Available: Details about estimation of molar absorption coefficient of polarons and transient absorption decays before and after the thermal annealing. This material is available free of charge via the Internet at http://pubs.acs.org.

JA9108787

(40) von Hauffa, E.; Parisi, J.; Dyakonov, V. *J. Appl. Phys.* **2006**, *100*, 043702.
(41) Mihailetchi, V. D.; Xie, H.; de Boer, B.; Koster, L. J. A.; Blom, P. W. M. *Adv. Funct. Mater.* **2006**, *16*, 699–708.